

ANTISENSE OLIGODEOXYNUCLEOTIDES FOR UROKINASE-PLASMINOGEN ACTIVATOR RECEPTOR HAVE ANTI-INVASIVE AND ANTI-PROLIFERATIVE EFFECTS *IN VITRO* AND INHIBIT SPONTANEOUS METASTASES OF HUMAN MELANOMA IN MICE

Silvia D'ALESSIO¹, Francesca MARGHERI¹, Marco PUCCI¹, Angela DEL ROSSO², Brett P. MONIA³, Mauro BOLOGNA⁴, Carlo LEONETTI⁵, Marco SCARSELLA⁵, Gabriella ZUPI⁵, Gabriella FIBBI^{1*} and Mario DEL ROSSO^{1*}

¹Department of Experimental Pathology and Oncology, University of Florence, Florence, Italy

²Department of Medicine, Section of Rheumatology, University of Florence, Villa Monnatessa, Florence, Italy

³Isis Pharmaceuticals, Carlsbad Research Center, Carlsbad, CA, USA

⁴Department of Experimental Medicine, University of L'Aquila Medical School, L'Aquila, Italy

⁵Regina Elena Cancer Institute, Experimental Chemotherapy Laboratory, Rome, Italy

We have targeted the urokinase-type plasminogen activator receptor (uPAR) with phosphorothioate antisense oligonucleotides (aODN) *in vitro* to evaluate the anti-invasive and anti-proliferative effects of uPAR down-regulation, as well as *in vivo* to evaluate anti-tumor and anti-metastatic activity. aODN-dependent uPAR downregulation *in vitro* was induced in cells of human melanoma, mammary carcinoma, ovarian carcinoma and SV-40-transformed embryonic lung fibroblasts. uPAR was determined by an antibody-based assay and by semiquantitative polymerase chain reaction. Cell invasion was evaluated by Matrigel invasion assay and cell proliferation by direct cell counting. aODN reduced uPAR, invasion and proliferation in all the treated cell lines. Following aODN treatment, human melanoma cells exhibited a strong decrease of uPAR-dependent ERK1/2 activation and were used *in vivo* to control metastasis in CD-1 male nude (nu/nu) mice by uPAR aODN injection. 60 mice were injected in the hind leg muscles with a suspension of 10⁶ melanoma cells. After 4 days, when a tumor mass of about 350 mg was evident in all the mice injected, 20 mice were treated *i.v.* with aODN and 20 with dODN at 0.5 mg/day for 5 consecutive days. Twenty control mice were not treated. A second and third cycle of treatment was administered at 2-day intervals. Treatment with aODN resulted into a 78% reduction of lung metastases and 45% reduction of the primary tumor mass with no loss of body weight. Our results suggest to evaluate the utility of uPAR aODN in controlling the metastatic spreading of human melanoma.

© 2004 Wiley-Liss, Inc.

Key words: antisense oligonucleotides; melanoma; metastasis; ERK; urokinase receptor (CD87)

The urokinase-type plasminogen activator (uPA) system consists of the serine-protease uPA, the plasminogen activator inhibitors type 1 and 2 (PAI-1, PAI-2) and the uPA receptor (uPAR). Two lines of evidence suggest a causal role for the uPA system in cancer invasion and metastasis: results from experimental model systems with animal tumor metastasis and the finding that high levels of uPA, PAI-1 and uPAR in many tumors predict poor patient prognosis. It is well documented that uPA and uPAR are overexpressed in malignant tumors and that these molecules are required for tumor invasion and metastasis.¹ The system does not support tumor metastasis by the unrestricted enzyme activity of uPA and plasmin (PL). The fibrinolytic system modulates cell adhesion by interactions of uPAR with vitronectin (VN), integrins and PAI-1, as well as cell invasion by extracellular matrix (ECM) degradation, in a sort of "grip-and-go" alternating cycles, which lead to cell movement.²

uPAR-bound pro-uPA can be activated to uPA by plasmin (PL), which is localized on plasminogen (PG) binding sites.² Trace amounts of PL activate pro-uPA to uPA and small amounts of uPA generate high local concentrations of PL, which degrades ECM both directly and indirectly by activation of pro-matrix metallo proteases (pro-MMPs).² Thus, a multi-enzyme proteolytic system

is assembled on the cell membrane, which is able to localize ECM degradation to specific pericellular sites and thereby to promote cell invasion into surrounding tissues. Moreover, there is evidence not only that uPA/uPAR interaction stimulates cell proliferation^{2,3} but also that high expression of uPAR alone regulates the rapid growth of human epidermoid carcinoma HEp3 *in vivo*, by interacting and activating $\alpha\beta$ 1-integrins, which trigger a signaling cascade that culminates in very strong and persistent ERK activation.⁴ Such an activation is mediated by ligand-independent activation of EGF receptor (EGFR)⁵ and is enhanced by uPA binding to uPAR and cell binding to fibronectin (FN).^{4,6} As a consequence, the constitutive ERK activation generated by uPAR overexpression keeps the signaling cascade for cell cycle progression on.⁷ Following uPAR down-regulation, ERK activity is lost, p38 becomes activated and the balance is shifted in favor of p38,⁷ which induces HEp3 cells to enter a state of cell dormancy.

Therefore, we believe that there is enough clinical and experimental background that suggests that impairment of uPAR expression may block cancer cell spreading. Several experimental models have shown that antisense oligodeoxyribonucleotides (aODN) are specific inhibitors of gene expression, which operate by means of a variety of mechanisms, all involving an aODN base pairing to the target mRNA.⁸ We have previously used uPAR-aODN to inhibit invasion of transformed human fibroblasts.⁹

In our study, we have used the aODN approach to inhibit expression of uPAR in a series of human transformed cell lines representing cancers of different origins. The results obtained *in vitro* have shown that aODN-mediated uPAR inhibition resulted in blockade of invasion and proliferation of all cell lines studied. Focusing our investigation on a human melanoma cell line (M20), which displays all the molecules of the fibrinolytic system typically associated to high aggressive behavior in this type of tumor, we have observed that aODN down-regulation of uPAR expres-

Grant sponsor: University of Florence; Grant sponsor: Ministero Istruzione, Università e Ricerca Scientifica (MIUR) (Progetti di Ricerca di Interesse Nazionale, PRIN); Grant sponsor: Ministero della Sanità, Associazione per la Ricerca sul Cancro (AIRC); Grant sponsor: Ente Cassa di Risparmio of Florence

*Correspondence to: Department of Experimental Pathology and Oncology of Florence University, Viale G. B. Morgagni, 50-50134 Florence, Italy. Fax: +39-055-4282-333. E-mail: delrosso@unifi.it or fibbi@unifi.it

Received 22 September 2003; Revised 14 November 2003; Accepted 21 November 2003

DOI 10.1002/ijc.20077

Published online 9 February 2004 in Wiley InterScience (www.interscience.wiley.com).

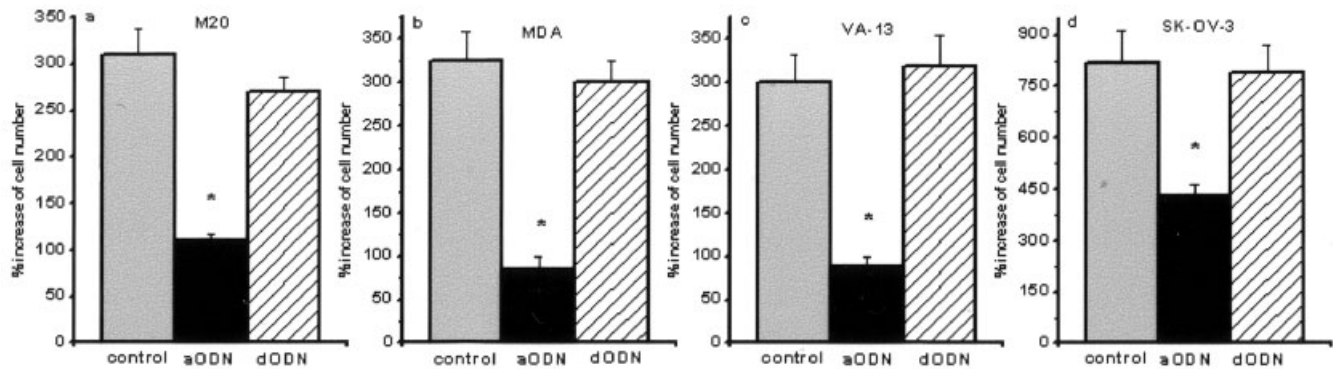
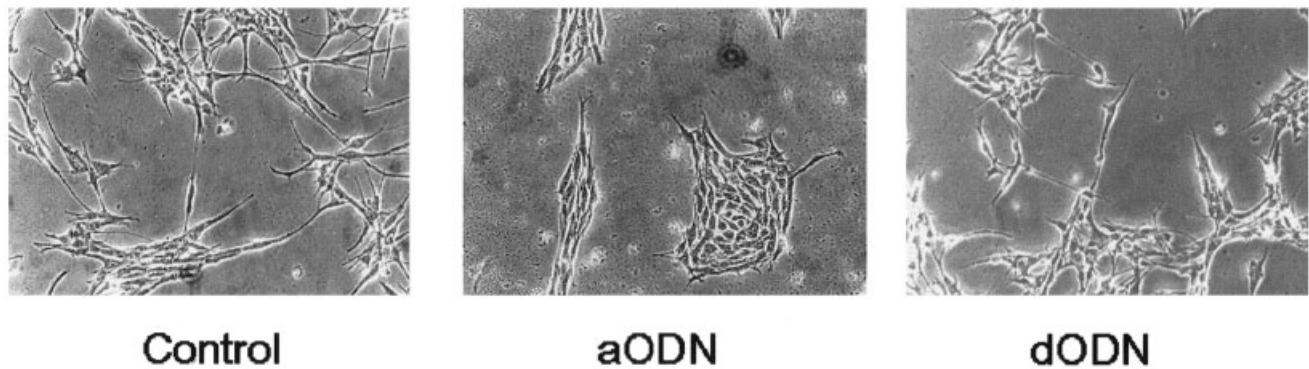
A**B**

FIGURE 1 – Effect of ODNs on proliferation of human malignant cell lines. (a) Values are expressed as the percent variation of cell number with respect to the initial number of plated cells. The original plating density varied for each cell line: 60×10^3 for the human melanoma cell line M20; 30×10^3 for MDA mammary carcinoma cells; 50×10^3 for the VA-13 transformed fibroblasts; 60×10^3 and 10^3 for the human ovarian carcinoma line SK-OV-3. Each value is the mean \pm SD of 3 different experiments performed in triplicate. * $p < 0.05$, significantly different from basal control. (b) Different pattern of human melanoma M20 cell growth in the presence of DOTAP (control), of uPAR aODN and dODN (magnification = $\times 200$).

sion inhibited ERK signaling. The use of anti-uPAR aODN in nude mice injected with the same melanoma cell line has exhibited a reduction of the primary tumor mass and a strong decrease of lung metastases.

MATERIAL AND METHODS

Cells

Human melanoma cell line M20 was derived from a metastasis of a patient with a cutaneous melanoma at Regina Elena Cancer Institute (Rome, Italy). After mechanical disaggregation of the biopsy fragment, the tumor line was maintained *in vitro* as monolayer culture in DMEM supplemented with 10% heat-inactivated fetal calf serum (FCS). The human ovarian carcinoma line SK-OV-3 was obtained from the Division of Cancer Treatment, Tumor Repository (National Cancer Institute, Frederick, MD) and was grown in DMEM supplemented with 10% FCS. MDA mammary carcinoma cells were kindly furnished by Dr. R. Giavazzi (Istituto Mario Negri, Bergamo, Italy), and were grown in DMEM with 10% FCS. The VA-13 cell line, the SV-40-transformed counterpart of WI-38 human embryonic lung fibroblasts, were purchased from Flow Laboratories (Milano, Italy) and cultured in DMEM with 10% FCS. VA-13 cells were obtained by infection of WI-38 fibroblasts with the transforming virus in the Wistar Institute (Philadelphia, PA) and were selected on the basis of fibrosarcoma production upon autologous and homologous implantation.¹⁰ All

the human tumoral cell lines were grown as monolayer cultures, their culture medium was supplemented with antibiotics and L-glutamine (2 mM) and cells were incubated at 37°C in a 5% CO₂-95% air atmosphere in a humidified incubator.

Invasion assays

The Boyden chamber was used to evaluate spontaneous invasion of untreated cells (control) and of cells treated with ODNs, as described.²⁴ The method is based on the passage of cells across porous filters separating the upper and lower wells of the migration chamber. We have used polyvinyl-pyrrolidone (PVP)-free polycarbonate filters, 8 μ m pore size. The filter was coated with the reconstituted basement membrane Matrigel (50 μ g/filter) (a kind gift of Dr. A. Albini, Genova, Italy). Control untreated cells and cells pretreated for 96 hr with ODNs as detailed below, were placed in the upper compartment of the Boyden chamber and migration was allowed to occur in the absence (control condition) or in the presence of ODNs in the medium of the upper and the lower compartment of the migration chamber. The chamber was incubated at 37°C for 6 hr and the filter was removed and fixed in methanol. Nonmigrating cells on the upper surface of the filter were removed with a cotton swab, while migrated cells, adherent on the lower filter surface, were stained with Diff-Quick (Mertz-Dade AG, Dade International, Milan, Italy) and counted by a light microscope ($\times 40$ in 10 random fields) per each well. Mobilization was measured by the number of cells moving across the filter. Each

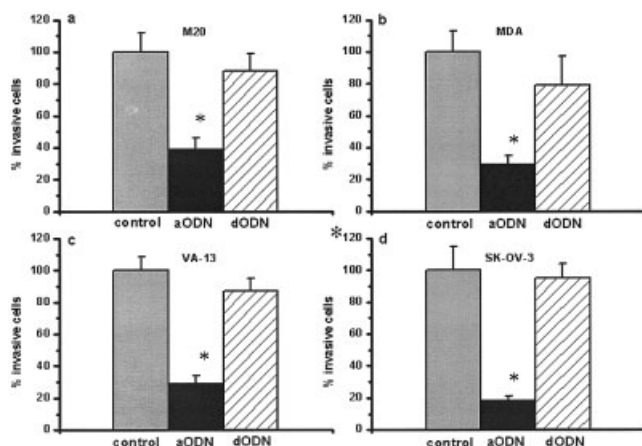


FIGURE 2 – Effect of ODNs on Matrigel invasion of human malignant cell lines. Values are expressed as the percent variation of cells adhering at the lower side of the migration filter in the presence of ODNs, with respect to the number of control untreated cells (DOTAP alone) taken as 100%. For each transformed cell line, 25×10^3 cells, pretreated for 96 hr with DOTAP alone or with ODNs, were placed in the upper well of the migration chamber and incubated at 37°C for 6 hr. The filter was then removed and fixed in methanol. At the end of incubation, the average number of invasive cells counted by a light microscope ($\times 40$ in 10 random fields) per each field, varied for each cell line. The values of invasive cells in untreated controls were 190 ± 12 for M14, 180 ± 15 for MDA, 270 ± 10 for VA-13 and 326 ± 18 for SK-OV-3. Each value is the mean \pm SD of 3 different experiments performed in triplicate. * $p < 0.05$, significantly different from basal control.

experimental point was performed in triplicate. Mean values of migrated cells for each point were calculated. Migration was expressed as mean \pm SD of the number of total cells counted/well or as the percentage of basal response.

Proliferation studies

Cell growth was quantified in subconfluent cell monolayers, as described.^{11,12} Cells were seeded onto 24-multiwell plates (Sarstedt, Verona, Italy) (the plating density varied for each cell line, as detailed in the legend to the figures) in medium supplemented with 10% FCS and were left to adhere overnight. Cells were then extensively washed in phosphate-buffered saline and maintained for 24 hr in serum-free DMEM. Medium was removed and cells were incubated with 10% FCS in DMEM, in the absence or in the presence of ODNs, as detailed below, as well as in the results and figure legends. Each experimental point was performed in triplicate. In M20 human malignant melanoma cells, proliferation was also evaluated in the presence of 1.5 mg/ml of anti-CD87 blocking monoclonal antibody (Mab CD87) (American Diagnostica, Greenwich, CT), which reacts with both occupied and unoccupied uPAR. At the end of the incubation, cells were detached with EDTA and counted with a cell counter. Data related to the effects of ODNs are expressed as percent of basal control, obtained in the absence of ODNs.

Detection of u-PA, u-PAR and PAI-1 transcripts by semi-quantitative RT-PCR and PCR products quantification

mRNA levels of uPAR, uPA and PAI-1 genes were determined by an internal-based semiquantitative reverse transcriptase-polymerase chain reaction assay (RT-PCR), as previously described.¹³ The uPAR gene primers were sense 5' -GGT CAC CCG CCG CTG- 3', antisense 5' -CCA CTG CGG TAC TGG ACA- 3'; the uPA gene primers were: sense 5' -AAA ATG CTG TGT GCT GCT GAC C- 3', antisense 5' -CCC TGC CCT GAA GTC GTT AGT G- 3'; the PAI-1 primers were: sense 5' -GAA CAA GGA TGA GAT CAG CAC C- 3', antisense 5' -ACT ATG ACA GCT

GTG GAT GAG G- 3'; the PAI-2 gene primers were: sense 5' -AAT GAA GTG GGA GCC AAT- 3', antisense 5' -GAG GAT CCT TAG GGT GAG CAA AA- 3'; the GAPDH gene primers were sense 5' -CCA CCC ATG GCA AAT TCC ATG GCA- 3', antisense 5' -TCT AGA CGG CAG GTC AGG TCC ACC- 3'. The expected size of cDNA fragments was 910 bp for u-PAR, 704 bp for uPA, 240 bp for tPA, 788 bp for PAI-1, 1,067 bp for PAI-2 and 598 bp for GAPDH. The ethidium bromide-stained cDNAs were photographed under a U.V. transilluminator by using Polaroid positive/negative instant films and quantified as reported elsewhere.¹³

Treatment with uPAR antisense oligodeoxyribonucleotide (aODN)

uPAR gene expression was inhibited with an 18-mer phosphorothioate aODN^{9,14} (ISIS Pharmaceuticals, Carlsbad Research Center, CA, product designation: ISIS 17916). The sequence of ISIS 17916 is 5' -CGG CGG GTG ACC CAT GTC -3'. As negative control, we used a completely degenerated 18-mer ODN (dODN): such ODN is a mixture of all the possible combinations of the bases that compose the aODN. ODN uptake and stability were enhanced by combining ODNs (10 $\mu\text{mol/L}$) with a cationic liposome (13 $\mu\text{mol/L}$), namely, DOTAP (Boehringer Mannheim, Mannheim, Germany), following the procedure previously described.⁹ Cell cultures were treated daily with ODNs for 4 days, on the basis of preliminary experiments indicating a steady-state reduction of uPAR number and of uPAR mRNA after 3 days of aODN treatment. Since the half-life of cationic lipid-combined ODNs in the culture medium was about 24 hr, the initial treatment with 10 μM cationic lipid-combined ODN was followed by a second addition of 5 μM after 24 hr in order to restore the initial concentration. On the fourth day, cells were counted, to evaluate the activity of the uPAR aODN on cell proliferation and were subjected to migration assay to evaluate the activity of the uPAR aODN on spontaneous invasion. In all the experiments performed with ODNs, we have supplemented cells with heat-inactivated serum (15 min at 65°C) in order to inactivate serum nucleases able to degrade the added compounds. For toxicity tests, the number of living cells (Trypan blue exclusion assay) was assessed at 12 hr intervals following ODN-DOTAP addition. Apart from a transient cell shrinkage occurring in the first 12 hr after addition of the compound, cell viability was unaffected.

u-PAR determination by ELISA assay

A monoclonal-antibody-based anti-uPAR assay (American Diagnostica) was used to measure uPAR number. Monolayers of control untreated cells and of cells treated with ODNs for 4 days, were lysed with lysis buffer, as suggested by the manufacturer, and an aliquot of the cell lysate was used for uPAR determination.

Western blotting

Control (DOTAP-treated), aODN and dODN-treated melanoma cells (M20) were counted for the indicated times, to evaluate the activity of the aODN anti-uPAR on cell proliferation, and were lysed in a 10 mM Tris-HCl buffer, pH 7.4, containing 150 mM NaCl, 1% Triton X-100, 15% glycerol, 1 mM sodium orthovanadate, 1 mM NaF, 1 mM EDTA, 1 mM phenylmethylsulfonyl fluoride and 10 μg of aprotinin per 100 ml. Protein concentrations were measured by the BCA protein assay reagent, using BSA as a standard. 40–100 μg of the cell extract protein was electrophoresed in SDS-12% polyacrylamide gel under reducing conditions and then blotted to a polyvinylidene difluoride membrane (Hybond-C Extra; Amersham Biosciences) for 3 hr at 35 V. The membrane was incubated with 5% skim milk in 20 mM Tris buffer, pH 7.4, for 1 hr at room temperature to block nonspecific binding and then probed with primary antibody to phospho-ERK (p42/p44) (Cell Signaling, Beverly, MA), ERK-2 (Santa Cruz Biotechnology, Santa Cruz, CA), p38^{MAPK} (Chemicon International, Temecula, CA), phospho-p38^{MAPK} (Biosource International, Camarillo, CA) proliferating cell nuclear antigen (PCNA)

TABLE I—u-PAR DETERMINATION (NG/MG PROTEIN) IN CONTROL AND ODNs-TREATED CELLS¹

Cell line	Control	aODN	dODN
M20	10.6 ± 0.9	2.76 ± 0.47*	8.7 ± 1.36
SK-OV-3	16.06 ± 1.8	4.41 ± 0.51*	13.65 ± 1.45
MDA	13.48 ± 1.21	3.30 ± 0.48*	11.66 ± 1.21
VA-13	18.01 ± 1.90	5.40 ± 0.71*	15.60 ± 1.60

¹Results are expressed as ng of u-PAR/mg of cell proteins. Each value represents the mean ± SD of 3 different determinations performed in triplicate in 3 different experiments. **p* < 0.05, significantly different from basal control.

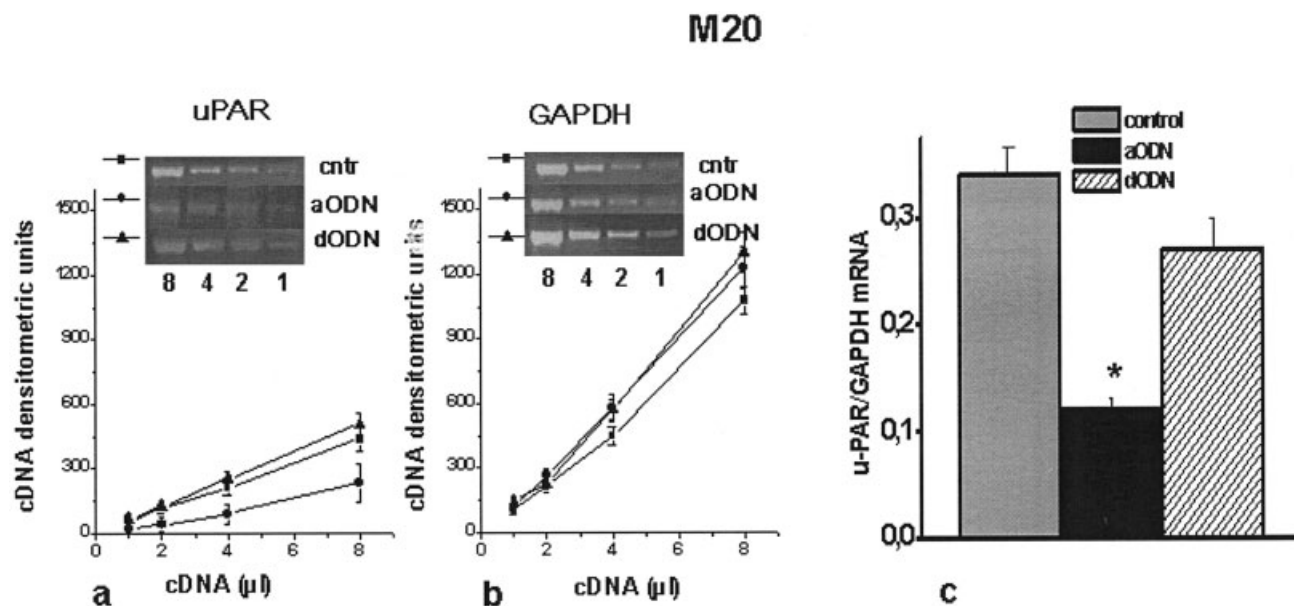


FIGURE 3—RT-PCR analysis. Expression of uPAR mRNA (a) and glyceraldehyde-3-phosphate dehydrogenase (GAPDH) mRNA (b). For the RT reaction, 1 μg of total RNA was isolated from control, aODN-treated and dODN-treated M20 melanoma cells. Aliquots of total cDNA were used to amplify uPAR and GAPDH with the indicated primers. After 25 cycles of PCR amplification, 10 μl aliquots were taken and separated on a 1% (w/v) agarose gel containing ethidium bromide (1 μg/ml). The PCR products were quantified densitometrically by a laser scanner. Inserts correspond to the ethidium bromide staining of the PCR products, which are numbered according to the μl of amplified cDNA. (c) Levels of uPAR mRNA in M20 cells. Three values of uPAR and GAPDH amplicates, falling within the range of linearity, were normalized to the total starting retrotranscripts volumes. Data are expressed as the ratio of uPAR mRNA/GAPDH mRNA. Data reported represent the mean ± SD of 3 determinations for each point. *At the 0.05 level of Student's *t*-test, the 2 means are significantly different.

(LabVision Corporation, Fremont, CA), uPAR, uPA and PAI-2 (American Diagnostica, Stamford, CT), PAI-1 (BioPool, Ventura, CA), tPA (kindly provided by Prof. P. De Petro, University of Brescia, Italy) overnight at 4°C. After incubation with horseradish peroxidase-conjugated donkey anti-mouse IgG (1:5,000) for 1 hr (Amersham Bioscience, Rainham, Great Britain), immune complexes were detected with the enhanced chemiluminescence ECL™ detection system (Amersham Bioscience). The membranes were exposed to autoradiographic films (Hyperfilm MP; Amersham Bioscience) for 1–30 min.

In vivo experiments

CD-1 male nude (nu/nu) mice, 6–8 weeks old and weighing 22–24 g, were purchased from Charles River Laboratories (Calco, Italy). A melanoma line with a high metastatic potential (M20), obtained from a metastasis of a patient from Regina Elena Institute, was employed. All procedures involving animals and their care were conducted in conformity with the institutional guidelines, which are in compliance with national (D.L. No. 116, G.U., Suppl. 40, Feb. 18, 1992; Circolare No. 8, G.U., July 1994) and international laws (EEC Council Directive 86/609, OJ L 358. 1, Dec 12, 1987; Guide for the Care and Use of Laboratory Animals, United States National Research Council, 1996). Each experimental group included 20 mice. To evaluate the antitumor efficacy of uPAR aODN, mice were injected in the hind leg muscles with a

cell suspension of 10⁶ M20 cells. Four days after cell implant a tumor mass of about 350 mg was evident in all the mice injected. Starting from this time mice were treated *i.v.* with aODN or dODN at 0.5 mg/day for 5 consecutive days, according to an administration schedule previously described for human melanoma xenografts in nude mice¹⁵ and on the basis of preliminary experiments indicating a significant reduction of human uPAR in the blood of aODN-treated animals after a single cycle of 5 days at 0.5 mg/day. A second and third cycle of treatment was administered at 2-day intervals. The tumor weight was calculated from caliper measurements according to Leonetti et al.¹⁵ To evaluate the metastatic potential of M20 melanoma, tumor bearing mice were sacrificed 25 days after tumor cell implantation, their lungs were removed and fixed in Bouin's solution to distinguish tumor nodules from lung tissue, and the number of metastases was evaluated under a stereomicroscope. Antitumor efficacy of treatments was assessed by the following end-points: i) percent tumor weight inhibition (TWI%), calculated as [1 – (mean tumor weight of treated mice/mean tumor weight of controls)] × 100; ii) T-C, median time (in days) for treated tumors (T) to achieve the size of 4,000 mg minus the time for untreated tumors (C) to achieve the same size and iii) reduction of lung metastases number. Moreover, all animals were subjected to necropsy and portions of various organs were processed for routine histological examination.

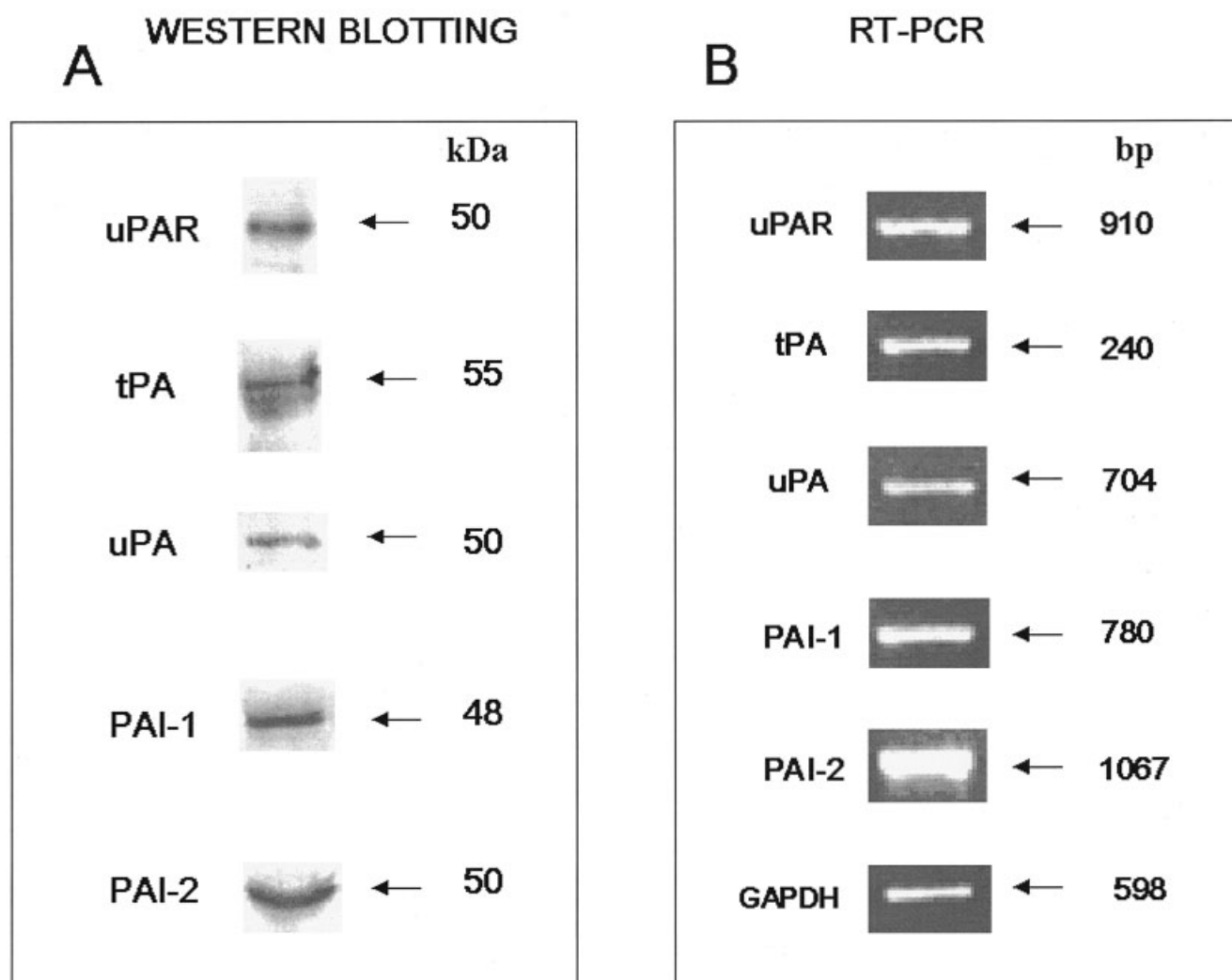


FIGURE 4—Characterization of the fibrinolytic system of M20 human melanoma cells. Western blots (a) and RT-PCR (b) showing the expression of uPAR, tPA, uPA, PAI-1 and PAI-2 in M20 human melanoma cells cultured *in vitro*. (a) Proteins (60 μ g) from cell lysates (uPAR), and culture medium (uPA, tPA, PAI-1 and PAI-2) were loaded in SDS-12% polyacrylamide gel under reducing conditions and blotted to a polyvinylidene difluoride membrane (Hybond; Amersham Biosciences). Immune complexes were detected with the ECLTM detection system (Amersham Biosciences). Arrows, positions of standards with known molecular weights. (b) Five micrograms of total RNA was reversely transcribed, and reversely transcribed DNA was then amplified, using indicated primers. GAPDH served as a control. Reaction products were analyzed by electrophoresis in 1% agarose gel containing ethidium bromide.

Statistical analysis

Results are expressed as means \pm SD for (*n*) experiments. Multiple comparisons were performed by the Student-Newman-Keuls test, after demonstration of significant differences among medians by nonparametric variance analysis according to Kruskal-Wallis. *In vivo* results were analyzed by the Mann-Whitney U test for statistical significance.

RESULTS

Activity of u-PAR aODN on proliferation of malignant cell lines

It is now well documented that both constitutive and growth factor-stimulated proliferation of normal cells, as well as the autocrine/paracrine-sustained growth of transformed cells, depend on the presence of a functionally available uPAR on the cell surface.^{1,12} Therefore, we have measured the cell proliferation rate in the absence and in the presence of uPAR aODN and dODN in the culture medium, as described above. In all the experiments described in the present and in the following paragraphs, the term

“control cells” refers to cells cultivated in the presence of DOTAP, since preliminary results have shown that the presence of the cationic phospholipid does not alter neither proliferation nor invasion of the malignant human cell lines under study. Figure 1a (a–d) shows the cell number reached in the growing plates by the various transformed cell lines under normal control conditions (10% FCS) and under the condition of uPAR expression inhibition by ODNs (10% FCS + dODN or aODN) after a 4 days daily treatment. It is evident that all the transformed cell lines respond to uPAR aODN with a striking decrease in their proliferation. The most dramatic antiproliferative activity was observed in the human breast carcinoma cells (MDA), human malignant melanoma cells (M20) and the transformed human fibroblasts (VA-13). Treatment with control dODN did not result in a decrease in cell growth. It is noteworthy that aODN treatment was also associated with a change of cell shape that was particularly evident in M20 malignant melanoma cells: cells exhibited an islet-like growth and cell shape changed from a stellate to a round morphology, which was not observed in dODN-treated cells (Fig. 1b). These results are in

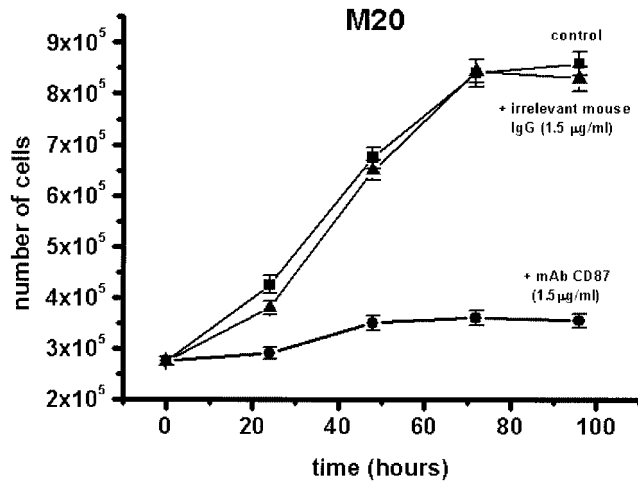


FIGURE 5—Proliferation pattern of M20 human melanoma cells; 60×10^3 M20 cells were plated in 6 well-multi-well plates in RPMI supplemented with 10% FCS. 48 hr later, when cells reached the number of about 2.5×10^5 /well, M20 monolayers were washed with PBS and added with RPMI-0.5% FCS, in the absence (control conditions) or in the presence of 1.5 $\mu\text{g}/\text{ml}$ anti-uPAR MAb CD87, or of 1.5 $\mu\text{g}/\text{ml}$ irrelevant mouse IgG. Results are the mean \pm SD of 3 experiments performed in duplicate.

agreement with previous observations indicating that uPAR, through its binding with VN and other partner proteins such as integrins, is related with reorganization of the actin cytoskeleton and induction of cell motility.^{16,17}

Activity of u-PAR aODN on invasion of malignant cell lines

Promotion of cell invasion has been considered the primary function of cell-associated uPAR. uPAR function in cell invasion has been shown to depend on either its property to mediate ECM destruction by its ligand uPA or on adhesive interactions of uPAR domain 2 and 3 with the ECM protein VN or PAI-1. On this basis, we expected to observe profound effects on cell invasiveness upon the u-PAR antisense. Each cell line was pretreated for 96 hr with ODNs as detailed in Material and Methods. Cells were then placed in the upper well of the Boyden chamber in the absence (control conditions) or in the presence of ODNs. Spontaneous invasion of Matrigel was evaluated after 6 hr. Figure 2 (a–d) shows the variation of Matrigel-invading cells, expressed as percent of control values. In order to reach and to spread on the bottom side of the filter, cells must invade the Matrigel layer, cross the filter pores and adhere to the lower aspect of the filter itself. Therefore, the number of cells counted in such a location reflects cell invasion. Results demonstrate that uPAR aODN treatment specifically and significantly impaired cell invasion of treated cells. Treatment with dODN produced a small nonspecific activity on cell invasion, which reached about 20% of invasion inhibition with respect to control untreated cells in the case of MDA breast cancer cells.

u-PAR expression is specifically affected by u-PAR aODN. To validate the activity of an antisense oligodeoxyribonucleotide, it is necessary to show specific inhibition of the expression of the protein encoded by the target mRNA. Therefore, we have performed ELISA assays on aliquots of the cell lysates in control cells and in ODNs-treated cells after daily addition of ODNs for 4 days, as detailed in Material and Methods. The data reported in Table I show that u-PAR aODN specifically reduced the cell-associated receptor, thereby accounting for the observed phenotypic effects.

Effect of ODNs on u-PAR mRNA levels

A segment of mRNA of the uPAR gene, including the aODN-targeted sequence, was reversely transcribed and amplified, as described under Material and Methods. For quantitation, PCR

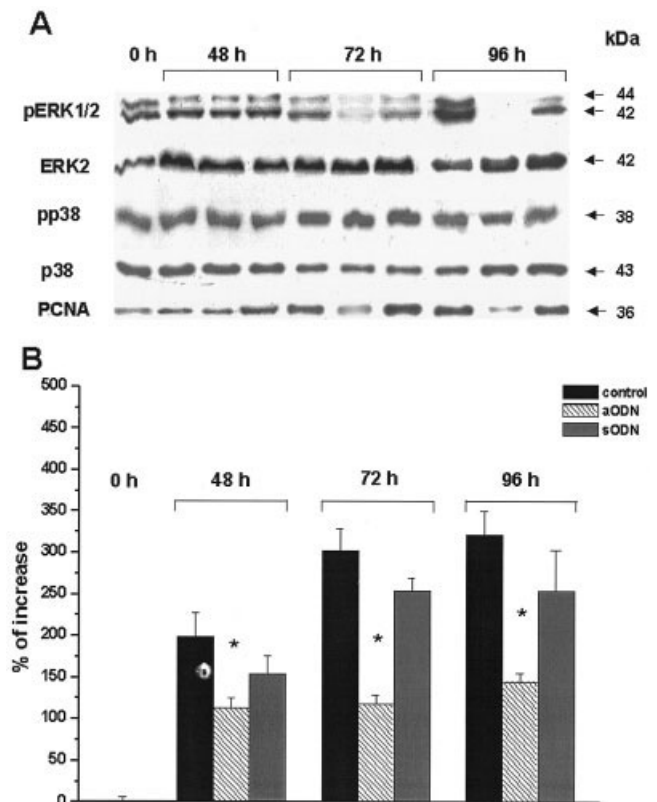


FIGURE 6—ODNs-dependent time kinetics of cell proliferation, p38^{MAPK} and ERK2 activation in M20 human melanoma cells; 60×10^3 M20 cells were plated in RPMI, supplemented with 10% FCS, for 48 hr until they reached the number of about 250×10^3 cells/well. At this time (0 hr) cell cultures were treated daily with ODNs for 4 days. At the indicated times, cells were counted to evaluate the activity of the uPAR aODN on cell proliferation (b) and were lysed to analyze ERK2 activation (phospho-ERK1/2 and pERK1/2), p38 activation (phospho-p38 and pp38), and PCNA expression by Western blotting (a), as indicated in Material and Methods. All columns represent the mean of triplicate measurements, and the error bars represent the S.D. * $p < 0.05$, significantly different from basal control.

values falling within the linearity range were normalized to that of the GAPDH gene, used as an internal standard. The treatment of cells with aODN resulted into a decrease of specific uPAR mRNA expression in all the treated cell lines. As an example, Figure 3 shows the results obtained in M20 human melanoma cells. Though even the dODN treatment resulted into a weak effect on uPAR mRNA, it is evident that the decrease obtained with aODN is mainly sequence specific. Similar results were obtained for the other malignant cell lines (not shown).

Characterization of the fibrinolytic system of M20 human melanoma cells to be used in vivo and activation of MAPK pathway

Since previous data had shown that plasminogen activators, their inhibitors and uPAR emerge in advanced stages of primary melanoma,¹⁸ that uPA positivity of cells of Spitz naevi may be suggestive of melanoma¹⁹ and that uPA, PAI-1 and PAI-2 may be considered as markers of stage I malignant melanoma,²⁰ we have characterized the fibrinolytic system of M20 human melanoma cells to be used for xenograft implants in nude mice. Figure 4a shows the Western blotting of uPAR in cell lysates, and of uPA, tPA, PAI-1 and PAI-2 in aliquots of M20 cells culture medium. Figure 4b shows the PCR products of the same molecules in total RNA extracts. It is evident that M20 cells produce all the components of the fibrinolytic system previously described in other

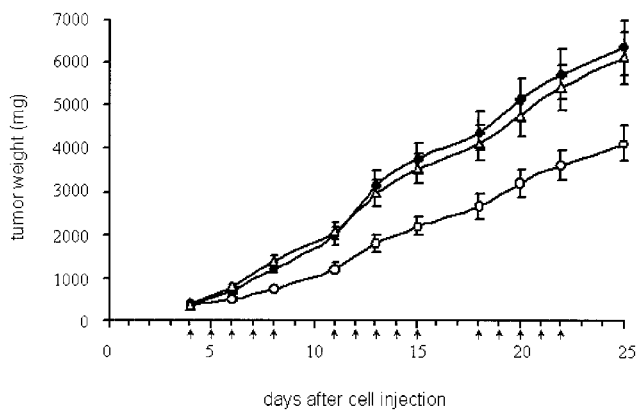


FIGURE 7 – Antitumor effect of ODNs administered *i.v.* on growth of M20 melanoma tumor implanted in nude mice. Mice were injected *i.m.* with 10^6 cells/mouse and starting from day 4 after cells injection they received ODNs at 0.5 mg/mouse/day for 5 consecutive days. A second and a third cycle were administered at 2-day intervals. (closed diamond), untreated; (open triangle), dODN; (open circle), aODN. The tumor weight inhibition of the aODN treated mice evaluated at nadir was 43%. Points are means (bars = SD). Arrows indicate the days of treatment.

human malignant melanoma-derived cell lines. However, the amount of uPA and tPA produced by M20 cells was very low, since zymography, performed on aliquots of culture medium, exhibited very weak lysis bands, even after 100-fold concentration (not shown). Figure 5 shows the kinetics of M20 cells proliferation in RPMI medium supplemented with 0.5% FCS, in the absence and in the presence of 1.5 $\mu\text{g/ml}$ anti-uPAR monoclonal antibody (MAb CD87), which interacts with both occupied and unoccupied uPAR and prevents uPAR interactions with integrins and vitronectin, thereby disrupting the mutual interactions among the molecules that constitute the ERK activating complex.²¹ Such MAb was able to impair M20 proliferation, indicating that in M20 cells uPAR is a key molecule that contributes to deliver mitogenic signals to the cell. On the basis of these result and of the data obtained with uPAR aODN on M20 and other malignant human cell lines, we have performed time kinetics of uPAR aODN activity on proliferation of M20 cells and on the regulation of ERK1/2, whose persistent activation (phospho-ERK1/2, pERK1/2) has been shown to constitutively depend on uPAR *per se*, as a critical component of the cell membrane-associated ERK-activating complex; 60×10^3 M20 cells were plated in 6-well multiwell plates, in RPMI supplemented with 0.5% FCS and left to grow for 48 hr, until they reached 2.5×10^5 cells/well. At this time (0 hr), cell cultures were treated with ODNs, as described, or with DOTAP alone (control conditions). Figure 6a shows the Western blotting of pospho-ERK1/2 and total ERK2, phospho-p38^{MAPK} and total p38^{MAPK}. It is evident that starting from 72 hr after uPAR aODN treatment (central lane of each triplet) ERK1/2 phosphorylation strongly decreases and is virtually absent after 96 hr, while p38^{MAPK} phosphorylation is unaffected. The proliferating cell nuclear antigen (PCNA) follows kinetics similar to ERK1/2 phosphorylation, as shown in the last line of Figure 6a. Figure 6b shows that proliferation of aODN-treated cells begins to decrease after 48 hr of treatment and is blocked since after 72 hr, while dODN exhibit only a weak effect. These data indicate that uPAR antagonization with MAb and uPAR expression inhibition may be sufficient to exert anti-proliferation effects on M20 cells and, together with the data on uPAR aODN inhibition of cell invasion, have prompted us to use M20 cells in *in vivo* xenograft experiments in nude mice to evaluate the antitumor activity of uPAR aODN.

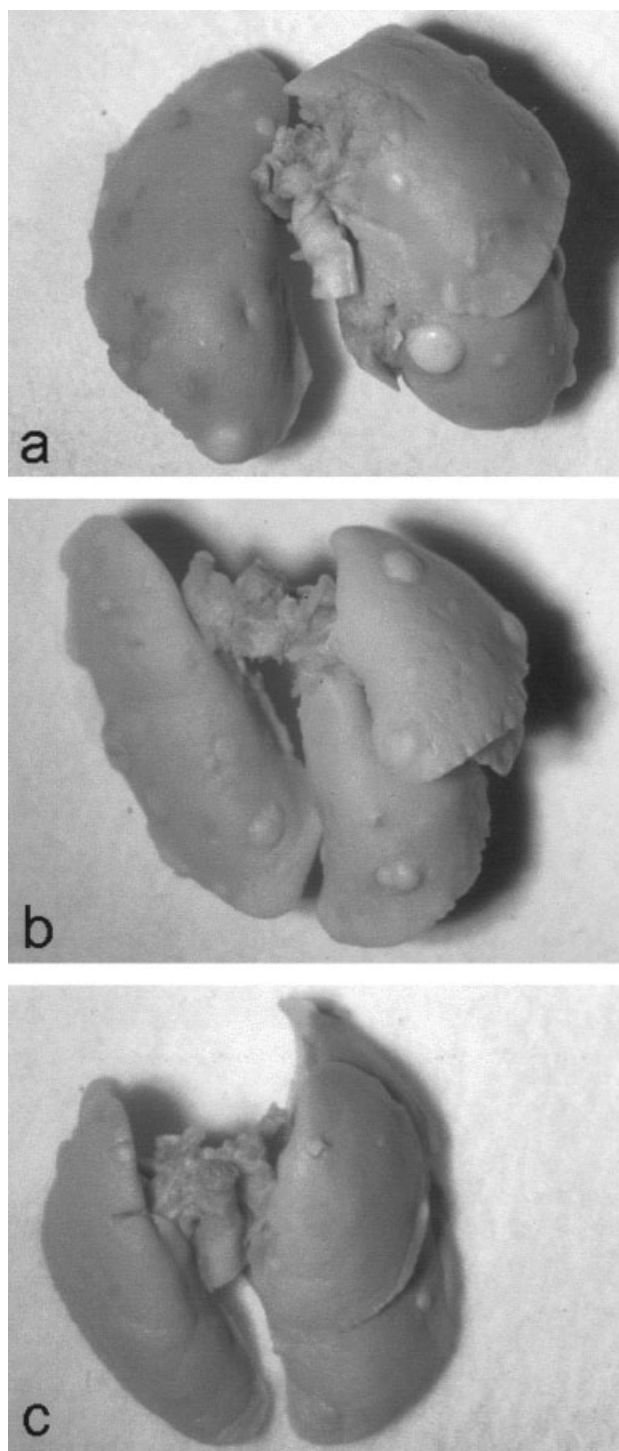


FIGURE 8 – Representative images of metastatic nodules in lungs from untreated (a), dODN (b) and aODN-treated mice (c). Lungs were removed and fixed in Bouin's solution to distinguish tumor nodules from lung tissue, and the number of metastases was evaluated under a stereomicroscope. In the shown side, the number of lung nodules are 20, 16 and 3 for untreated, dODN and aODN-treated mice. Equivalent number of metastases were counted in the not shown side of lungs.

In vivo antitumor activity of u-PAR aODN

Nude mice bearing M20 tumors were treated with aODN or dODN at 0.5 mg/day/mouse for 5 consecutive days. Three cycles of administration were injected at 2-day intervals.¹⁵ As shown in

Figure 7, a reduction of the tumor growth was observed after aODN treatment, while dODN did not affect the growth of tumor. In particular a reduction of a tumor mass of 43% was observed after the 2nd cycle of administration and a delay of 8 days to reach the weight of 4,000 mg was detected. This effect was accompanied by a significant reduction of lung nodules. Figure 8 shows representative lungs of mice sacrificed at the 25th day of tumor growth. Lungs from the aODN-treated mouse (c) show no more than 3 metastases, while lungs from the dODN (b) and untreated mice (a) show about 16 and 20 lung nodules, respectively. Moreover, it was evident that a larger mass of metastatic nodules was present in the dODN and untreated mice relative to the aODN-treated group. The count of lung metastatic nodules of 20 mice for each group demonstrated that the median number of lung metastases was significantly different ($p < 0.001$) between aODN-treated mice (lung nodules 7, range 1–21) and untreated (lung nodules 45, range 24–73) or dODN treated mice (lung nodules,³³ range 22–70). While no significant difference ($p = 0.29$) was observed between untreated and dODN treated group. Routine histological examination of other organs (lymphnodes and liver) did not show the presence of metastatic nodules in various groups (control, dODN and aODN). Finally, the treatment was well tolerated.

DISCUSSION

We have shown that aODN against uPAR mRNA impair invasion and proliferation of several human tumor cell lines *in vitro*, representing cancers of different origins. Using a human melanoma tumor line that shows a high metastatic potential *in vivo*, we demonstrate that uPAR aODN reduce the tumor growth and the number of spontaneous lung metastases. These results, are in agreement with our previous data,^{22,23} showing the efficacy *in vivo* of ODNs, in combination with anti-neoplastic drugs, in improving the response of human melanoma. The melanoma cells used in our study (M20), express uPAR, uPA, tPA, PAI-1 and PAI-2, the full range of the so-called “cell-associated fibrinolytic system,” suggestive of highly aggressive tumors, as previously reported.^{18–20} Previous data on M14 human melanoma cells have indicated that the mitogenic effect of uPA is independent from the high affinity binding to uPAR.²⁴ In M20 cells, we have observed that uPAR *per se*, besides its involvement in cell invasion, delivers mitogenic signals independently of its stimulation with uPA, as previously observed for other malignant cells.^{4–7} Although these data do not exclude the possibility of a mitogenic activity of uPA, dependent on its interaction with binding molecules other than uPAR and/or with uPAR itself, they suggest that impairment of uPAR expression has the chance to control not only invasion but also proliferation of human melanoma cells. Such uPA-independent uPAR activity is mediated by the constitutive ERK activation generated by uPAR and is blocked by uPAR down-regulation with aODN, which is paralleled by inhibition of ERK1/2 phosphorylation. Recently, it has been shown that a balance that favors p38 activation over ERK can induce a persistent growth suppression in high malignant human carcinoma cells *in vivo*.⁷ Following uPAR down-regulation, ERK activity is lost, p38 becomes activated and the balance is shifted in favor of p38.⁷ This observation has been extended to several malignant cell lines,²⁵ but a human melanoma cell line was an exception to the rule. This cell line exhibits a high ERK activity but also a high p38 activity and the ratio between ERK and p38 is unbalanced in favor of p38. Nonetheless, it is highly tumorigenic and metastatic. As a consequence, the negative feed-back exerted by p38 on ERK activity, which leads to growth suppression in other malignant cell lines, does not seem to work in

these human melanoma cells. The mechanism responsible for the negative feed-back from p38 to ERK is still unknown, but some reports suggest that the p38 pathway may be dysfunctional in melanomas.^{26,27} As a confirmation of these results, we found no evidence of increase of p38 activity upon uPAR aODN down-regulation of ERK phosphorylation. Therefore, it is evident that downregulation of uPAR and the subsequent downregulation of ERK activity is sufficient to induce growth suppression in human melanomas.

Inhibition of uPAR can provide an anti-invasive strategy in pathologies where invasion is a pivotal pathogenic event.²⁸

In vivo, the methods based on inhibition of uPAR by an “outside-in” approach (monoclonal or polyclonal serotherapy, antagonists of uPAR interactions) may potentially suffer from some drawbacks, such as the relatively low amount of the injected antibody that actually arrives to the tumor and the poor diffusion of immunoglobulins throughout large tumor masses. Moreover, antibodies can be inhibited or scavenged by soluble antigens (soluble uPAR is often a marker of tumor burden), which can bind to their combining site and prevent attachment to the relevant antigen on the cell surface. uPAR antagonists should be able to impair the multiple interactions of uPAR with uPA, vitronectin, integrins, PAI-1 and high molecular weight kininogen (all activities intrinsically related to uPAR function in the “grip-and go” regulation of cell invasion), without exerting any agonistic effect on uPAR, such as chemoinvasion and proliferation^{29–31} on the base of structural similarities with the ligand molecule to be displaced.

The “inside-out” approach, based on aODN, allows to by-pass such complications. aODNs have been successfully applied to inhibit uPAR expression *in vitro* and *in vivo*, using either the classic aODN technology, which consists of the injection of antisense DNA strands complementary to uPAR mRNA,^{9,32} or the antisense RNA technology, based on cell transfection with a vector capable of expressing the antisense transcript complementary to uPAR mRNA.^{33,34} In both cases, a reversion of the invasive phenotype of the malignant cells was obtained. However, since the use of viral or plasmid delivery vectors may potentially suffer from little target cell specificity, insertional mutagenesis and difficulties encountered in large-scale production for clinical trials,³⁵ and RNA molecules, administered from outside or generated by vector transfection, are very sensitive to nucleases and have half lives of 15 to 30 min in the serum,³⁵ we have chosen to use the classical aODN approach.

We have shown for the first time that “knock-down” of uPAR gene expression obtained with aODN inhibits growth and metastasis of malignant human melanoma cells in nude mice. Although our data might be exhaustive only for melanoma cells, there is the possibility that other human tumors that mainly rely on the uPAR system for their constitutive growth and invasion could respond to uPAR aODN treatment *in vivo*, as preliminarily indicated by data obtained *in vitro* in the present work on other human malignant cell lines.

ACKNOWLEDGEMENTS

We are indebted to Dr. A. Albini, Istituto Nazionale per la Ricerca sul Cancro (IST), c/o Centro di Biotecnologie Avanzate, Genova, Italy, for providing us with Matrigel. We also acknowledge the skillful technical assistance of Mr. M. Cutri of the Department of Experimental Pathology and Oncology (University of Florence) with computer programs.

REFERENCES

- Andreasen PA, Egelund R, Petersen HH. The plasminogen activation system in tumor growth, invasion, and metastasis. *Cell Mol Life Sci* 2000;57:25–40.
- Mignatti P, Rifkin DB. Nonenzymatic interactions between protein-
- and the cell surface: novel roles in normal and malignant cell physiology. *Adv Cancer Res* 2000;78:103–57.
- Del Rosso M, Fibbi G, Pucci M, D'Alessio S, Del Rosso A, Magnelli L, Chiarugi V. Multiple pathways of cell invasion are regulated by

- multiple families of serine proteases. *Clin Exp Metastasis* 2002;19:193–207.
4. Aguirre Ghiso JA, Kovalski K, Ossowski L. Tumor dormancy induced by down-regulation of urokinase receptor in human carcinoma involves integrin and MAPK signalling. *J Cell Biol* 1999;147:89–104.
 5. Liu D, Aguirre Ghiso JA, Estrada Y, Ossowski L. EGFR is a transducer of the urokinase receptor initiated signal which is required for *in vivo* growth of a human carcinoma. *Cancer Cell* 2002;1:445–57.
 6. Aguirre Ghiso JA. Inhibition of FAK signalling activated by urokinase receptor induces dormancy in human carcinoma cells *in vivo*. *Oncogene* 2002;21:2513–24.
 7. Aguirre Ghiso JA, Liu D, Mignatti A, Kovalski K, Ossowski L. Urokinase receptor and fibronectin regulate the ERK (MAPK) to p38 (MAPK) activity ratios that determine carcinoma cell proliferation or dormancy *in vivo*. *Mol Biol Cell* 2001;12:863–79.
 8. Tamm I, Dorken B, Hartman G. Antisense therapy in oncology: new hope for an old idea? *Lancet* 2001;358:489–97.
 9. Quattrone A, Fibbi G, Anichini E, Pucci M, Zamperini A, Capaccioli S, Del Rosso M. Reversion of the invasive phenotype of transformed human fibroblasts by anti-messenger oligonucleotide inhibition of urokinase receptor gene expression. *Cancer Res* 1995;55:90–5.
 10. Jensen F, Koprowsk H, Pagano JS, Ponten J, Ravdin RG. Autologous and homologous implantation of human cells transformed by simian virus 40. *J Natl Cancer Inst* 1964;32:917–37.
 11. Fibbi G, Caldini R, Chevanne M, Pucci M, Schiamone N, Morbidelli L, Parenti A, Granger HJ, Del Rosso M, Ziche M. Urokinase-dependent angiogenesis *in vitro* and diacylglycerol production are blocked by antisense oligonucleotides against the urokinase receptor. *Lab Invest* 1998;78:1109–19.
 12. Fibbi G, Pucci M, Grappone C, Pellegrini G, Salzano R, Casini A, Milani S, Del Rosso M. Functions of the fibrinolytic system in human Ito cells and its control by basic fibroblast and platelet-derived growth factor. *Hepatology* 1999;29:868–78.
 13. Fibbi G, Barletta E, Dini G, Del Rosso A, Pucci M, Cerletti M, Del Rosso M. Cell invasion is affected by differential expression of the urokinase plasminogen activator/urokinase plasminogen activator receptor system in muscle satellite cells from normal and dystrophic patients. *Lab Invest* 2001;81:27–39.
 14. Roldan AL, Cubellis MV, Masucci MT, Behrend N, Lund LR, Dano K, Appella E, Blasi F. Cloning and expression of the receptor for human urokinase plasminogen activator, a central molecule in cell-surface plasmin-dependent proteolysis. *EMBO J* 1990;9:467–74.
 15. Leonetti C, D'Agnano I, Lozupone F, Valentini A, Geiser T, Zon G, Calabretta B, Citro GC, Zupi G. Antitumor effect of c-myc antisense phosphorothioate oligodeoxynucleotides on human melanoma cells *in vitro* and *in mice*. *J Natl Cancer Inst* 1996;88:419–29.
 16. Kjoller L, Hall A. Rac mediates cytoskeletal rearrangements and increased cell motility induced by urokinase-type plasminogen activator receptor binding to vitronectin. *J Cell Biol* 2001;152:1145–1157.
 17. Kjoller L. The urokinase plasminogen activator receptor in the regulation of the actin cytoskeleton and cell motility. *Biol Chem* 2002;383:5–19.
 18. de Vries TJ, Quax PH, Denijn M, Verrijp KN, Verheijen JH, Verspaget HW, Weidle UH, Ruiter DJ, van Muijen GN. Plasminogen activators, their inhibitors, and urokinase receptor emerge in late stages of melanocytic tumor progression. *Am J Pathol* 1994;144:70–81.
 19. Ferrier CM, Van Geloof WL, Straatman H, Van De Molengraft FJ, Van Muijen GN, Ruiter DJ. Spitz naevi may express components of the plasminogen activation system. *J Pathol* 2002;198:92–99.
 20. Stabuc B, Markovic J, Bartenjev I, Vrhovec I, Medved U, Kocijancic B. Urokinase-type plasminogen activator and plasminogen activator inhibitor type 1 and type 2 in stage I malignant melanoma. *Oncol Rep* 2003;10:635–39.
 21. May AE, Schmidt R, Kanse SM, Chavakis T, Stephens RW, Schomig A, Preissner KT, Neumann F-J. Urokinase receptor surface expression regulates monocyte adhesion in acute myocardial infarction. *Blood* 2002;100:3611–17.
 22. Citro G, D'Agnano I, Leonetti C, Perini R, Bucci B, Zon G, Calabretta B, Zupi G. c-myc antisense oligodeoxynucleotides enhance the efficacy of cisplatin in melanoma chemotherapy *in vitro* and *in nude mice*. *Cancer Res* 1998;58:283–89.
 23. Leonetti C, Biroccio A, Benassi B, Stringaro A, Stoppacciaro A, Sempile SC, Zupi G. Encapsulation of c-myc antisense oligodeoxynucleotides in lipid particles improves antitumoral efficacy *in vivo* in a human melanoma line. *Cancer Gene Ther* 2001;8:459–68.
 24. Koopman JL, Slomp J, de Bart ACW, Quax PHA, Verheijen JH. Mitogenic effect of urokinase on melanoma cells are independent of high affinity binding to the urokinase receptor. *J Biol Chem* 1998;273:33267–72.
 25. Aguirre-Ghiso JA, Estrada Y, Liu D, Ossowski L. ERKmapk activity as a determinant of tumor growth and dormancy; regulation by p38SAPK. *Cancer Res* 2003;63:1684–95.
 26. Korabiowska M, Betke H, Kellner S, Stachura J, Schauer A. Differential expression of growth arrest, DNA damage genes and tumor suppressor gene p53 in nevi and malignant melanomas. *Anticancer Res* 1997;17:3697–3700.
 27. Korabiowska M, Brinck U, Kotthaus I, Berger H, Droese M. Comparative study of the expression of DNA mismatch repair genes, the adenomatous polyposis coli gene and growth arrest DNA damage genes in melanoma recurrences and metastases. *Melanoma Res* 2000;10:537–44.
 28. Del Rosso M, Fibbi G, Pucci M, Matucci Cerinic M. Antisense oligonucleotides against the urokinase receptor: a therapeutic strategy for the control of cell invasion in rheumatoid arthritis and cancer. *Clin Exp Rheumatol* 1998;16:389–93.
 29. Rabbani SA, Desjardins J, Bell AW, Banville D, Mazar A, Henkin J, Goldtzman, D. An amino-terminal fragment of urokinase isolated from a prostate cancer cell line (PC-3) is mitogenic for osteoblast-like cells. *Biochem Biophys Res Commun* 1990;173:1058–64.
 30. Resnati M, Guttinger M, Valcamonica S, Sidenius N, Blasi F, Fazioli F. Proteolytic cleavage of the urokinase receptor substitutes for the agonist-induced chemotactic effect. *EMBO J* 1996;15:1572–82.
 31. Anichini E, Zamperini A, Chevanne M, Caldini R, Pucci M, Fibbi G, Del Rosso M. Interaction of urokinase-type plasminogen activator with its receptor rapidly induces activation of glucose transporters. *Biochemistry* 1997;36:3076–83.
 32. Shetty S, Kumar A, Johnson AR, Idell S. Regulation of mesothelial cell mitogenesis by antisense oligonucleotides for the urokinase receptor. *Antisense Res Dev* 1995;5:307–14.
 33. Kook YH, Adamski J, Zelent A, Ossowski L. The effect of antisense inhibition of urokinase receptor in human squamous cell carcinoma on malignancy. *EMBO J* 1994;13:3983–91.
 34. Go Y, Chintala SK, Mohanam S, Gokaslan Z, Venkaij B, Bjerkgvig R, Oka K, Nicolson GL, Sawaya R, Rao JS. Inhibition of *in vivo* tumorigenicity and invasiveness of a human glioblastoma cell line transfected with antisense uPAR vectors. *Clin Exp Metastasis* 1997;15:440–6.
 35. Kufe DW, Advani S, Weichselbaum R. Principles of gene therapy. In: Bast RC, Kufe DW, Pollock RE, Weichselbaum R, Holland JF, Frei E, eds. *Cancer medicine e.5*. Hamilton, Ontario: BC Decker, Inc., 2000. 876–89.